Fluid-dynamic and thermo-mechanical analyses of the Monoblock Mitre Bend for the ITER Electron Cyclotron Upper Launcher

Avelino Mas Sánchez[a*], Rene Chavan[b], Davide Dall'Acqua[c], Mario Gagliardi[c], Timothy Goodman[b], Jose Pacheco Cansino[c], Eduardo Rodriguez Ordoñez[a], Gabriella Saibene[c], Paul Wouters[c]

[a] *Department of Construction and Manufacturing Engineering, University of Oviedo, E-33203 Gijón, Spain*
[b] *Ecole Polytechnique Fédérale de Lausanne (EPFL), Swiss Plasma Center (SPC), CH-1015 Lausanne, Switzerland*
[c] *Fusion for Energy, Josep Pla 2, Torres Diagonal Litoral B3, E-08019 Barcelona, Spain*

The ITER Electron Cyclotron Heating (ECH) system will be used to counteract magneto-hydrodynamic plasma instabilities by aiming up to 20 MW of mm-wave power at 170 GHz. The primary vacuum boundary at the Electron Cyclotron Upper Launcher (EC UL) extends into the port cell region through eight beamlines, defining the so-called First Confinement System (FCS). Each beamline, designed for the transmission of 1.31 MW, is delimited by the closure plate at the port plug back-end and by a diamond window in the port cell. The FCS essentially consists of a Z-shaped set of straight corrugated waveguides (WG) connected by Mitre Bends (MB) with a nominal inner diameter of 50 mm.

Due to the space restrictions, the eight MBs at the last FCS section are grouped into two monoblocks. Each Monoblock Mitre Bend (MBMB) consists of a body with corrugated feedthroughs defining a specific angle for each beamline and four mirrors attached by bolted connection to reflect the mm-wave power. The thermal expansion arising from the ohmic losses, the cooling pressure, the bolt pre-tension and the imposed displacements coming from the connection with the transmission lines are the primary design loads for the MBMBs. The fluid-dynamic analyses performed for both upper and lower MBMBs show that highest temperature takes place in the MB mirrors, reaching a maximum value of 203°C at the beam center. The thermo-mechanical analyses demonstrate that the peak stress also occurs at this location with a maximum value of 324 MPa. These stresses are categorized and compared with the allowable limits defined in the ASME code, what probes that the current design of both upper and lower MBMBs are able to withstand the loads taking place during the mm-wave normal operation.

Keywords: ITER; ECH; Upper Launcher; Mitre Bend; Waveguides

1. Introduction and background

The four ITER Electron Cyclotron Upper Launchers (EC UL, [1]) will be used to drive current locally in order to stabilize neoclassical tearing modes. The mm-wave components in the eight beamlines of each EC UL are divided into essentially quasi-optical in-vessel and guided-wave ex-vessel assemblies. The ex-vessel waveguide (WG) components, extending the primary vacuum boundary of the port plug into the port cell region on both sides of the bioshield wall, are part of the First Confinement System (FCS, Fig. 1) for which, ITER SIC-1 requirements apply. Each transmission line (TL) of the FCS, designed for the transmission of 1.31 MW of mm-wave power at 170 GHz, is delimited by the closure plate sub-plate, with a WG feedthrough and by a diamond window in the port cell (an intermediate isolation valve provides the double containment).

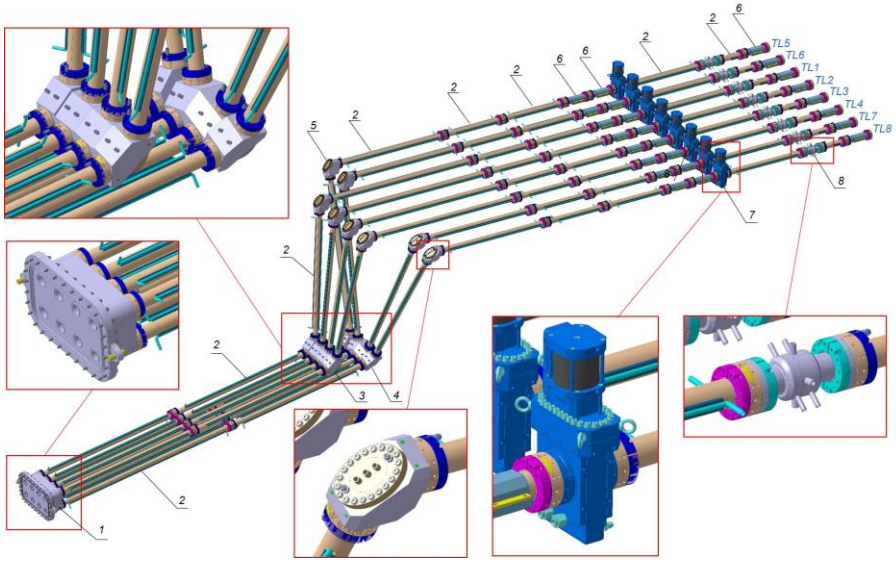

Fig. 1. Current state of the First Confinement System. 1. Closure plate sub-plate, 2. Standard WGs, 3. Upper MBMB, 4. Lower MBMB, 5. MBs, 6. Clamped WGs, 7. Isolation valves, 8. Diamond windows

author's email: amassanchez@gmail.com

The beam line is comprised of a Z-shaped set of straight corrugated WGs with a nominal inner diameter of 50 mm and connected by Mitre Bends (MB). Due to the space restrictions, the last eight MBs of the FCS section (nearest the torus) are grouped into two Monoblock Mitre Bends (MBMB). Recently, the FCS layout has changed to ensure a maintenance corridor (the MBs relative to TL1, TL2, TL3 and TL4 moved forwards, whereas the MBs relative to TL5, TL6, TL7 and TL8 moved backwards), resulting in a modification of the angles of the quasi-vertical WGs connected to the MBMBs. This new configuration required a redesign of both upper and lower MBMBs.

2. Design description

Each MBMB (Fig. 2) consists of a body with corrugated feedthroughs defining a specific angle (approximately 100°) for each beamline, and four mirrors attached by bolted connection to reflect the mm-wave power. Both MBMB bodies and MB mirrors are made of CuCrZr in order to minimize the ohmic losses and to improve the heat distribution during mm-wave power transmission.

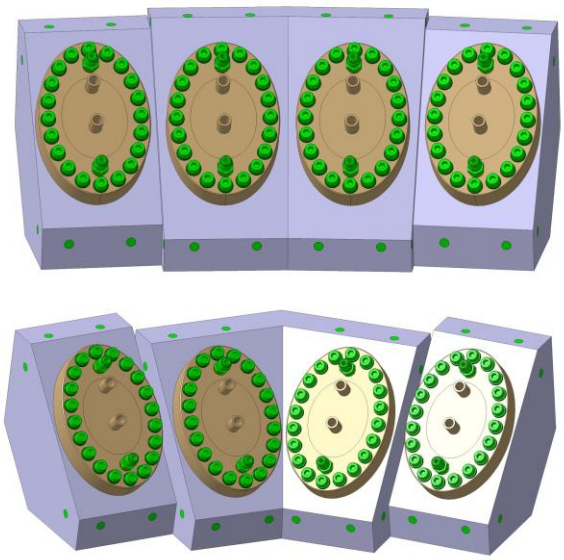

Fig. 2 Current design of the upper MBMB (top) and lower MBMB (bottom)

In order to comply with ITER SIC-1 requirements, the mechanical couplings between MB mirrors, as well as WGs, with each MBMB body shall contain two concentric metallic seals with two leak testing access ports between the seals (sniffers). The necessary force to compress the metallic seals is provided by 12 and 20 M8 bolts for each WG flange coupling (circular seals) and each mirror coupling (elliptical seals), respectively. Threaded inserts are included in the MBMB body design so the suitable pre-tension value can be reliably applied.

2.1 MB mirrors

Several cooling MB mirror designs were assessed in the past [2]. The cooling design analyzed in this paper (Fig. 3) consists in a one inlet/outlet circuit with a spiral shape and square cross-section of 5x10 mm. The inlet is slightly shifted to one side to guarantee full-developed flow at the location of higher power density. These cooling channels will be milled and subsequently covered by HIP (Hot Isostatic Pressing) or diffusion bonding techniques (both techniques are compatible with [3]).

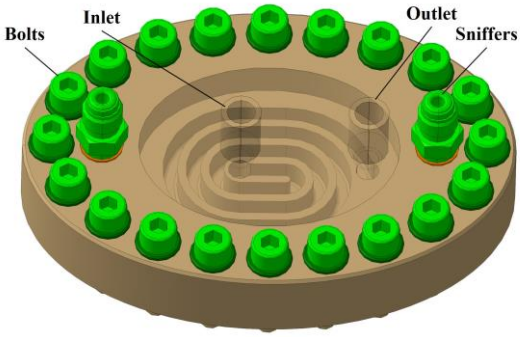

Fig. 3 Spiral cooling channel design of the MB Mirror

2.2 MBMB bodies

The cooling channels for the MBMB bodies are performed by drilling (8 mm diameter). The distance between the axes of the WG feedthroughs and cooling channels is fixed to 32 mm (minimum thickness of about 3 mm) to maximize the heat dissipation. The holes left by the drilling operations are covered by cooling caps and welded through a three-step procedure that allows the full penetration welding. All the welded connections are designed to take into account the full penetration butt welds required in [3]. Four inlets/outlets are defined, as these cooling circuits are connected in series with the rest of components of the same beamline.

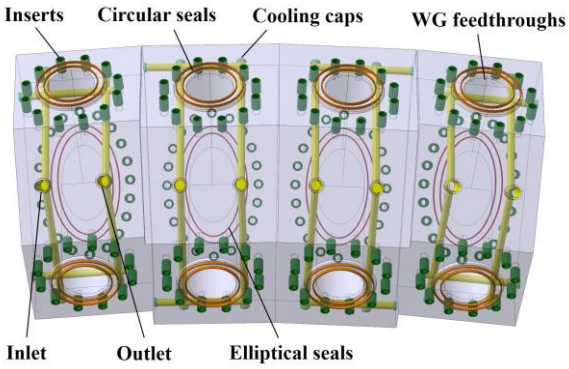

Fig. 4 Cooling design for the upper MBMB body

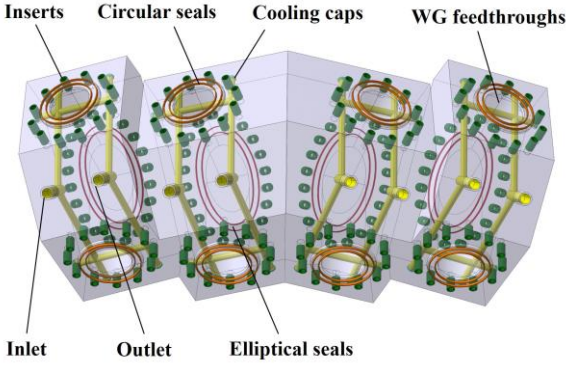

Fig. 5 Cooling design for the lower MBMB body

3. Fluid-dynamic analyses

Two independent steady-state fluid-dynamic simulations are performed in ANSYS Workbench 19.2 CFX [4] in order to assess the flow distribution and heat transfer taking place in both upper and lower MBMBs during nominal mm-wave normal operation. These analyses aim to assess if the assigned mass flow rate to each component produces an acceptable temperature rise while maintaining an admissible pressure drop through the cooling channels.

3.1 Model description

3.1.1 Geometry and mesh

The geometry considered in the analyses covers both MB mirrors and MBMB bodies. Components that are not relevant for the thermal performance such as bolts, sniffers, inserts or metallic seals are removed from the model. Some features such as boltholes or small chamfers were also simplified. Symmetry conditions are applied to limit the computational cost. The cooling fluid is obtained by a boolean operation based on the above-mentioned geometries.

The fluid domain is meshed with 10 inflation layers on the surfaces in contact with the solid domain in order to properly simulate the viscous sub-layer. The first inflation layer height is $5 \cdot 10^{-6}$ m, which leads to a y^+ value smaller than 1 near the walls for the whole domain. The overall number of nodes considered in the numerical model is 2965548 and 2870954 for the upper and lower MBMB simulations, respectively.

3.1.2 Material properties and turbulence model

The properties related to CuCrZr alloy [5] are applied as temperature-dependent correlations to the MB mirrors and MBMB bodies. Water properties at 34°C and 1 MPa (CCWS-1 inlet properties [6]) are considered for the fluid domain. The turbulence model selected for this analysis is the Shear Stress Transport since this model typically provides good results for cases in which there is a high heat transfer between the solid and the cooling fluid.

3.1.3 Boundary conditions

The inlet cooling conditions of the CCWS-1 cooling system (34°C and 1 MPa [6]) are considered for the fluid-dynamic analysis of both upper and lower MBMB. The assigned mass flow rate is 0.15 kg/s and 0.27 kg/s for the MB mirrors and MBMB bodies, respectively.

A fraction of the beam power will be lost on the mirror surface during the beam propagation. The fractional loss power can be calculated for each beam according the following equation (worst-case polarization):

$$f_{\Omega i} = 4S\sqrt{\frac{\pi\rho_e}{\lambda Z_0}}\left(\frac{1}{\cos\frac{\theta}{2}}\right) \qquad (1)$$

Where ρ_e is the electrical resistivity of the CuCrZr [3] at 200°C, S is an enhancement factor of absorption on mirrors due to surface roughness and other imperfections (S=1.5 for MB mirrors), λ is the wavelength for 170 GHz (0.00176 m), Z_0 is the impedance of free space (~120π Ohm) and θ is the full reflection angle for each beam.

The absorbed power for each mirror can be calculated as:

$$q(r) = \frac{P_0 \cdot f_{\Omega i} \cdot 3.71 \cdot \cos\frac{\theta}{2}}{\pi a^2} \cdot J_0^2\left(2.405\frac{r}{a}\right) \qquad (2)$$

Where P_0 is the input power (1.31 MW [6]), a is the waveguide radius (0.025 m), 3.71 comes from the mode normalization, J_0 is the Bessel function of order 0, 2.405 is the first 0 of J_0 and r is equal to $\sqrt{x^2 + y^2}$ (x and y being the coordinates in the plane transverse to the waveguide axis).

Eq. 2 produces a power density peak of 5.94 MW/m^2 [7] on the MB mirror reflecting surface (Fig. 6). The total absorbed power is 4.9 kW for each mirror. In addition, a uniform value of 10.2 kW/m^2 [7] coming from the ohmic attenuation and the High Order Modes (HOM) is applied on the MBMB feedthroughs, which contributes with another 0.35 kW for each beamline.

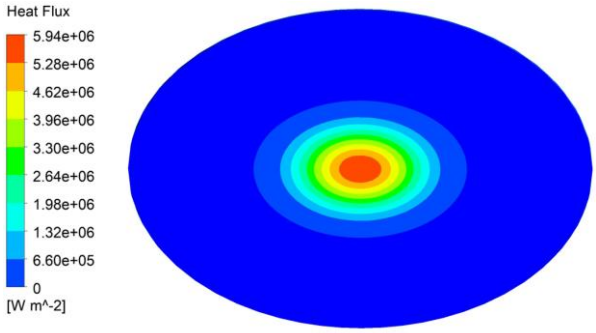

Fig. 6 Power density on the MB mirrors

3.2 Results

3.2.1 Temperature distribution

The highest temperature is located in the MB mirrors (Fig. 7), reaching a maximum value of 203°C at the beam center (the temperature is very similar for every MB mirror, less than 1°C). Both upper and lower MBMB bodies present temperature values considerably lower (Fig. 8 and Fig. 9), with maximum values of around 50°C at the contact region with the MB mirrors.

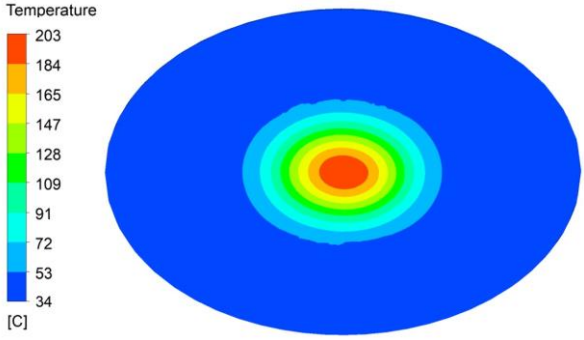

Fig. 7 Temperature distribution on the MB mirrors

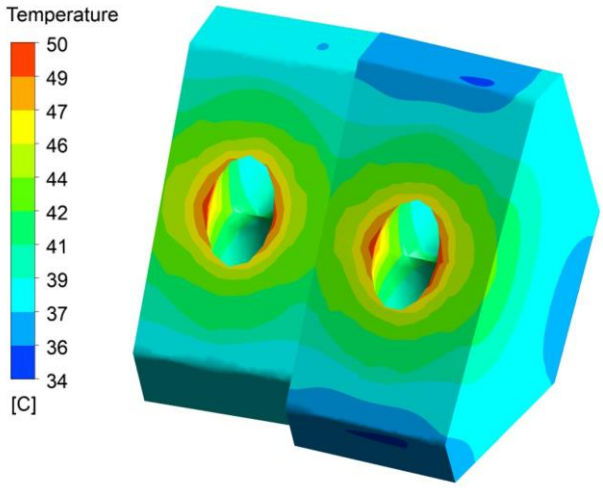

Fig. 8 Temperature distribution on the upper MBMB body

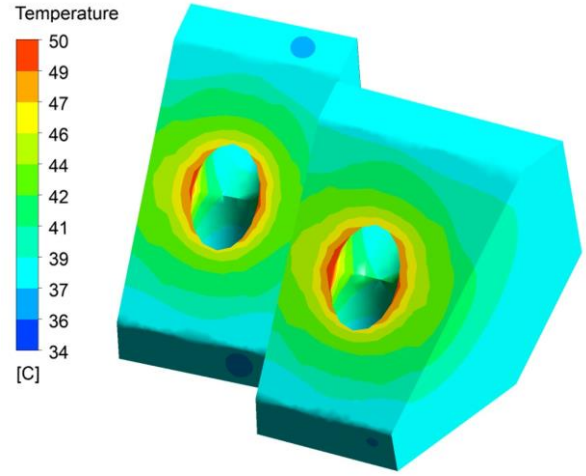

Fig. 9 Temperature distribution on the lower MBMB body

The outlet temperature for the water is 40.1°C and 34.7°C respectively for the MB mirror and MBMB bodies (each channel), which is smaller than the maximum allowed outlet temperature for the CCWS-1 circuit (64°C [6]), and therefore, allows their connection in series with other ex-vessel components. The maximum local temperature of the cooling water is 134°C and 38°C respectively for the MB mirror and MBMB, which is lower than the boiling temperature at 0.45 MPa (minimum allowable pressure at the CCWS-1 circuit [6]), avoiding possible cavitation issues.

3.2.2 Pressure drop and flow velocity

The pressure drop is 0.24 bars and 0.18 bars for each MB mirror and each MBMB body circuit, respectively. These values are admissible compared with the maximum allowed pressure drop for the CCWS-1 circuit (5.5 bars [6]). Therefore, these values also justify their possible connection in series with other actively cooled ex-vessel components.

The maximum velocity values are 6.9 m/s and 4.8 m/s for the MB mirrors and MBMB bodies. These values are acceptable for the ex-vessel components (no reducing-oxidizing conditions as for the In-Vessel components occurs) so no erosion/corrosion issues are expected.

4. Thermo-mechanical analyses

Two independent steady-state thermo-mechanical analyses are performed in ANSYS Workbench 19.2 Static Structural [4] in order to assess the upper and lower MBMBs in terms of plastic collapse and ratchetting against the loads taking place during the mm-wave normal operation. These numerical analyses provide the stress distribution, which will be post-processed and subsequently compared with the allowable design limits available in the fabrication codes.

4.1 Model description

4.1.1. Geometrical model and mesh

The geometrical model (Fig.10) used for the upper and lower MBMBs simulations cover the MB mirrors, MBMB bodies and the adjacent WGs. Bolts, inserts and simplified metallic seals are also included in order to simulate the pre-tension process. Some components, e.g. sniffers, which are not relevant for the mechanical performance, are removed from the assembly. Symmetry conditions are also used to reduce the computational cost of the simulation.

The metallic seals are modelled as prismatic rings with square cross sections of 1 mm width (estimated contact surface after compression) and 2.6 mm height (seal cross section diameter before compression) for both circular (WG) and elliptical (mirror) seal sets (2 per location). An initial separation between faces (0.47 mm, seal compression recommended by the supplier) is defined as the starting state of the model in order to properly simulate the bolt pre-tensioning process. The seal properties definition and the loading strategy used in this simulation are the ones developed in [8].

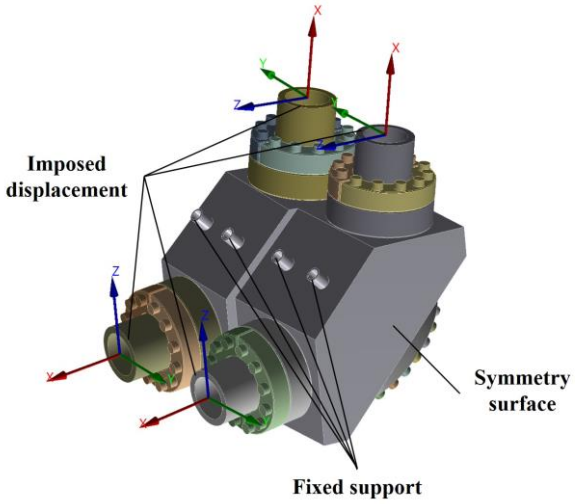

Fig. 10 Geometrical model of the upper MBMB thermo-mechanical analysis (the same approach is followed for the lower MBMB)

A uniform element size value of 3 mm is applied to the MB mirrors and bolting, while a value of 6 mm is considered for the MBMB bodies and attached WGs (the element size is reduced to 3 mm at the regions close to the contacts). The overall number of elements defined in

the numerical models are 1071584 and 860852 for the upper and lower MBMBs, respectively.

4.1.2. Material properties

The temperature-dependent material properties used in this analysis are obtained from [5]. The material properties related to CuCrZr alloy are applied to the MB mirrors, MBMB bodies and WGs while Inconel 718 properties are used for the bolting (bolts, compression rings and inserts). The material behavior for these materials is considered as linear. Non-linear hysteresis curves [8] are introduced to simulate the seals behavior (same curves are used for both circular and elliptical seals).

3.1.3. Contacts

Frictional contacts (friction coefficient = 0.2) are defined between the surfaces defining a coupling such as MB mirrors and WGs with the MBMB bodies) and between MB mirror bolts and WG compression rings with their respective seating surfaces.

3.1.4. Boundary conditions and loads

The analysis setup is divided into 6 sequential load steps (Table 1). This strategy not only aims to facilitate the convergence of the numerical problem, but also to assess the independent contribution of each load step.

In the first load step the model fixed supports are defined at the MBMB body cooling pipes boundaries while a pre-tension load of 14 kN is applied to each bolt (12 bolts for each flange coupling and 20 bolts for each mirror coupling). The gravity, the CCWS-1 inlet pressure (1 MPa, [6]) on the wetted surfaces, and the temperature distribution are applied on the second, third and fourth load steps, respectively. In addition, the imposed displacement coming from the vacuum vessel movement and waveguide thermal expansion are applied in the fifth load step. A value of (0.13, 021, 0.03) mm (local WG coordinate system, Fig.10) is applied to the WG borders (values obtained from the overall simulation of the EC UL FCS during normal operation [9]). Finally, the fixed support at the MBMB body cooling pipes is released in the sixth load step (since the model is already constrained by the imposed displacements at the WG boundaries).

Table 1. Load steps

Load step	Fixed support	Pre-tension each bolt (kN)	Gravity (m/s)	CCWS-1 cooling pressure (MPa)	Temp. field (°C)	Imposed displacement (mm)
1	ON	14	OFF	OFF	OFF	OFF
2	ON	Lock	ON	OFF	OFF	OFF
3	ON	Lock	ON	1	OFF	OFF
4	ON	Lock	ON	1	Fig. 7, 8 and 9	OFF
5	ON	Lock	ON	1	Fig. 7, 8 and 9	(0.13, 0.21, 0.03)
6	OFF	Lock	ON	1	Fig. 7, 8 and 9	(0.13, 0.21, 0.03)

4.2 Results

4.2.1 Stress intensity

The design-by-analysis rules developed in the ASME code section III [10] are prescribed for the design validation of the MBMBs. These rules are based on the maximum shear stress theory. Therefore, the stress results obtained from these simulations shall be assessed in terms of stress intensity (Tresca) in order to be compared with the allowable limits.

Fig. 11 shows the stress intensity field in the most stressed MB mirror. The stress peak is located at the mirror center (where the highest temperature occurs) reaching up to 324 MPa. The stress values among the different MB mirrors are very close to each other since their temperature distributions are very similar.

Regarding the MBMB bodies (Fig. 12 and 13), the highest stresses take place in the region of bolted connection, reaching maximum values of 154 MPa and 145 MPa for the upper and lower MBMB bodies, respectively. Comparing these stress distributions with the ones obtained in the MB mirrors, it can be seen that the stress in MBMB bodies is much lower, since the temperature values are also lower.

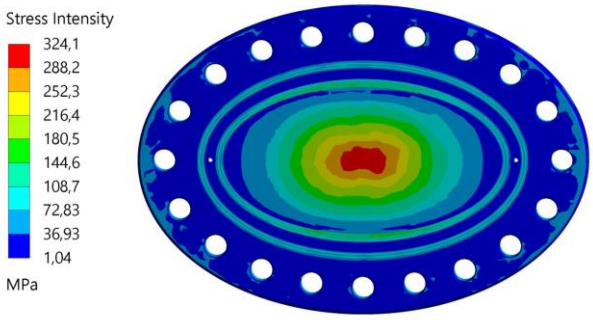

Fig. 11 Stress intensity field in the most stressed MB mirror

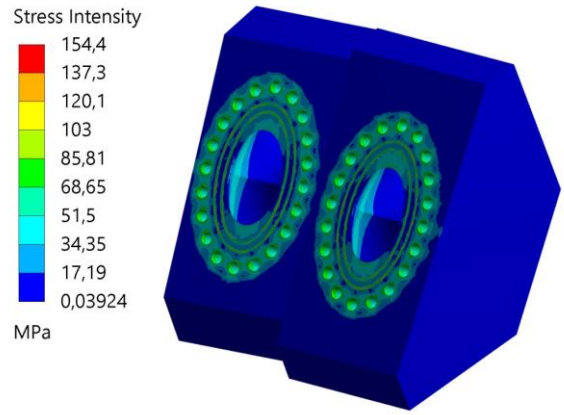

Fig. 12 Stress intensity field in the upper MBMB body

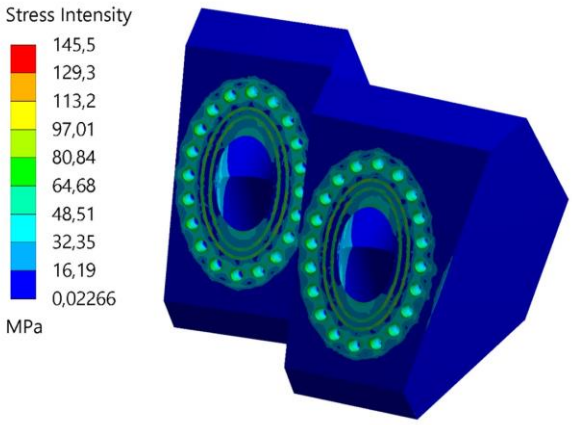

Fig. 13 Stress intensity field in the lower MBMB body

4.2.2 Structural integrity assessment

The elastic stress analysis method is considered for the protection assessment against plastic collapse and ratcheting. In this method the stresses are computed using an elastic analysis, classified into categories, and limited to allowable values that have been conservatively established such that a plastic collapse or ratcheting will not occur. The stress categorization is obtained by linearizing the stress (membrane, bending and peak) along the so-called Stress Classification Lines (SCLs). These lines shall be defined through the entire thickness of the considered section and normal to the midline.

To evaluate protection against plastic collapse the following three criteria shall be satisfied:

$$P_m \leq S_m \qquad (3)$$

Where P_m is the general primary membrane equivalent stress and S_m is the design stress intensity.

$$P_L \leq S_{PL} \qquad (4)$$

Where P_L is the local primary membrane equivalent stress (primary membrane equivalent stress when close to discontinuities) and S_{PL} is computed as the larger of the quantities shown below:

- 1.5 times the design stress intensity (S_m)
- The yield strength (S_y). The previous value shall be used when the ratio of the minimum specified yield strength to the ultimate tensile strength (S_u) exceeds 0.70 or the value of S_m is governed by time-dependent properties

$$P_L + P_B \leq S_{PL} \qquad (5)$$

Where $P_L + P_B$ is the primary membrane (general or local) plus the primary bending equivalent stress.

To evaluate protection against ratcheting the following limit shall be satisfied:

$$\Delta S_{n,k} \leq S_{PS} \qquad (6)$$

Where $\Delta S_{n,k}$ is the equivalent stress range derived from the combination of general or local primary membrane stresses plus primary bending stresses plus secondary stresses ($P_L + P_B + Q$) and S_{PS} is computed as the larger of the quantities shown below:

- 3 times the design stress intensity (S_m)
- 2 times the yield strength (S_y). The previous value shall be used when the ratio of the minimum specified yield strength to the ultimate tensile strength (S_u) exceeds 0.70 or the value of S_m is governed by time-dependent properties

The most stressed cross-section takes place at the MB mirror center (Fig. 14). The allowable values for CuCrZr at 200°C are 86 MPa, 155 MPa and 310 MPa for S_m, S_{PL} and S_{PS}, respectively. Table 2 reports the verifications performed for each SCL. The comparison between the categorized stress and the allowable design limits according to ASME code shows that the MBMB design is capable of withstanding the expected loads taking place during normal operation.

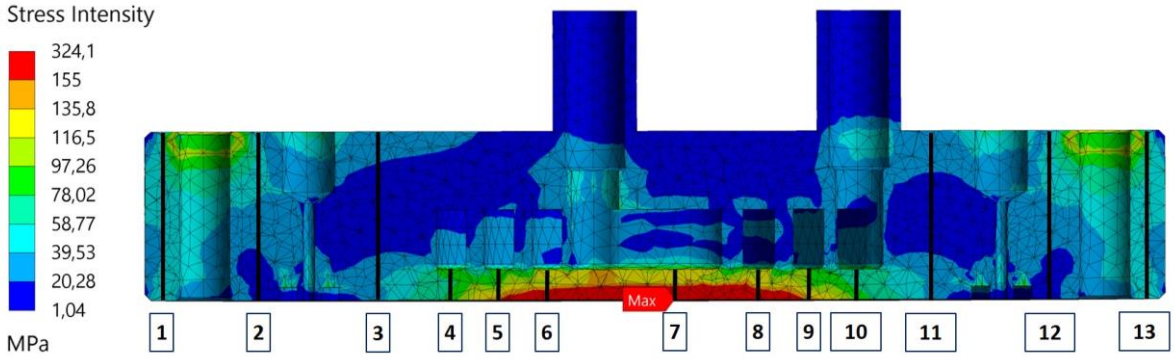

Fig. 14 SCLs for stress verification on the MB mirror

Table 2. MB mirror stress verification (values in MPa)

SCL	1	2	3	4	5	6	7	8	9	10	11	12	13	Limit
P_m	46.5	32.6	4.1	19.1	19.4	20.6	21.7	20.5	20.3	20.3	4.3	32.4	48.6	86
P_L	-	-	-	-	-	-			-	-	-	-	-	155
$P_L + P_B$	58.3	64.1	25.8	21.3	25.7	27.7	27.1	26.8	25.4	20.9	29.8	62.8	61.1	155
$\Delta S_{n,k}$	59.9	70.4	41.0	82.3	145.3	197.9	277.9	194.6	132.6	85.5	33.1	69.1	63.6	310

5. Conclusions

A modified mechanical design concept of both upper and lower Monoblock Mitre Bends, capable of fulfilling the requirements in terms of safety, vacuum tightness, space restriction, mm-wave transmission, cooling capability and mechanical integrity has been proposed in this paper.

The fluid-dynamic analyses show that the power deposited in both MB mirrors and MBMB bodies during the normal operation scenario can be properly removed with an acceptable mass flow, resulting in an admissible pressure drop and maximum local temperature of the cooling water lower than the boiling temperature at this pressure.

The thermo-mechanical analyses demonstrate that the highest stress occurs at the MB mirror center, location of the temperature peak (beam center). The comparison between the classified stress and the allowable design limits according ASME code shows that the design of both upper and lower MBMB is capable of withstanding, in terms of plastic collapse and ratcheting, the mechanical and thermal stresses developed during the normal operation scenario.

Additional analyses shall be performed in order to validate the MBMBs design against the full range of load combinations expected to take place throughout the system life-cycle [6].

Acknowledgments

The work leading to this publication has been funded by Fusion for Energy under the expert contracts F4E-2019-EXP-332 and F4E-2019-EXP-340. This publication reflects the views only of the author, and Fusion for Energy cannot be held responsible for any use which may be made of the information contained therein.

References

[1] D. Strauss, et al., Nearing final design of the ITER EC H&CD Upper Launcher, Fusion Eng. Des. 146, Part A (2019) 23-26

[2] P. Santos, et al., Thermal mechanical analyses of the mm-wave miter bend for the ITER electron cyclotron upper launcher first confinement system, Fusion Eng. Des. In Press, 136, Part A (2018) 650-654

[3] L. Worth, ITER Vacuum Handbook, ITER_D_2EZ9UM v2.5 (2019)

[4] http://www.ansys.com/

[5] J. Campbell et al, ITER Material Properties handbook properties, ITER_D_2239QQ v1.0 (2005)

[6] N. Casal, EC UL Sub-System Load Specification [SSLS-52.UL], F4E_D_25QD28 v5.1 (2018)

[7] T. Goodman, ECH UL millimeter waveguide thermal loading, F4E_D_2JUYRJ v1.1 (2019)

[8] A. Mas Sánchez, et al., Mechanical analyses of the waveguide flange coupling for the first confinement system of the ITER electron cyclotron upper launcher, Fusion Eng. Des. 109-111, Part A, (2016) 532-538

[9] A. Mas Sánchez, et al., Mechanical analyses of the ITER electron cyclotron upper launcher first confinement system, Fusion Eng. Des. In Press, 123 (2017) 458–462

[10] ASME Boiler & Pressure Vessel Code, Section III, Division 1, Subsection NC – Class 2 Components (2010)